Int. J. Electrochem. Sci., 12 **(2017)** 4351 – 4359, doi: 10.20964/2017.05.32

International Journal of
ELECTROCHEMICAL
SCIENCE
www.electrochemsci.org

Short Communication

BiOCl Nanoplates Decorated on g-C_3N_4 for Enhanced Photocatalytic Activities

Yongkui Huang[1], *Shifei Kang*[2,*], *Wenpeng Gong*[3], *Yao Fang*[1], *Hengfei Qin*[1], *Siyu Liu*[1], *Shuijin Yang*[3], *Xi Li*[1,*]

[1] Department of Environmental Science and Engineering, Fudan University, Shanghai 200433, China
[2] School of Environment and Architecture, University of Shanghai for Science and Technology, Shanghai 200093, China
[3] Hubei Collaborative Innovation Center for Rare Metal Chemistry, College of Chemistry and Chemical Engineering, Hubei Normal University, Huangshi 435002, China
[*]E-mail: xi_li@fudan.edu.cn, sfkang@usst.edu.cn

Received: 29 November 2016 / *Accepted:* 11 March 2017 / *Published:* 12 April 2017

A facile solvothermal method has been successfully developed for the preparation of BiOCl/g-C_3N_4 nanocomposite using sodium dodecyl benzene sulfonate as the surfactant. The results revealed that BiOCl nanoplates with thickness below 5 nm and widths of 20~30 nm were uniformly dispersed on the surface of g-C_3N_4 nanosheets, indicating the formation of a close contact between the BiOCl and g-C_3N_4. The catalytic activity of the obtained BiOCl/g-C_3N_4 composite has been evaluated by the degradation process of rhodamine B under visible light irradiation. It has been demonstrated that the catalytic activity of BiOCl/g-C_3N_4 composite was significantly enhanced compared with the bare component due to the synergistic effect between BiOCl and g-C_3N_4.

Keywords: g-C_3N_4; BiOCl; Nanocomposite; Surfaces; Photocatalyst

1. INTRODUCTION

As a green technology, photocatalysis is attracting considerable interests because of its great potential in resolving the environmental and energy problems [1, 2]. The traditional semiconductor material (such as TiO_2, ZnO) areworked only under the ultraviolet light radiation owing to their wide bandgap [1, 3]. Recently, the scientists have devoted a lot of efforts to the design and development of novel photocatalysts to meet the requirements of commercial application [4-6]. As a novel semiconductor, bismuth oxychloride (BiOCl) has drawn much attention owing to its high photocatalytic performances [7, 8]. BiOCl was used as catalysts in the photodegradation of organic

pollutants, which exhibited superior activity to commercial P25 [9, 10]. However, BiOCl has poor photocatalytic activity because its bandgap is about 3.5 eV[10]. To overcome this drawback, many strategies have been proposed to amend the catalytic performances of BiOCl materials.

Recently, graphitic carbon nitride (g-C_3N_4) has been extensively studied on the field of photocatalysis because of its suitable band energy, 2D layered nanostructure, high thermal and chemical stability [4, 11, 12]. Several groups have reported on the preparation of BiOCl-based g-C_3N_4 materials to achieve a high photocatalytic activity [13, 14]. However, the particle size of BiOCl is a few hundreds of nanometers, and heterojunctions with intimate contacts between the BiOCl and g-C_3N_4 can't be constructed, which is crucial for their practical applications [10, 15]. Therefore, it is of significance to design an effective approach to enlarge the contact area and form a perfect interface between BiOCl and g-C_3N_4.

Herein, uniform BiOCl decorated on the surface of g-C_3N_4 composites have been obtained through a facile solvothermal reaction with sodium dodecyl benzene sulfonate (SDBS) as the surfactant. The SDBS was used to reduce the size of BiOCl nanocrystals and simultaneously increase their uniformity. The BiOCl nanoplates were uniformly adhered on the surface of g-C_3N_4, indicating that a close contact was formed between the BiOCl and g-C_3N_4, which could promote the charge transfer between BiOCl and g-C_3N_4. The experimental results demonstrated that the BiOCl/g-C_3N_4 is an excellent photocatalyst for the degradation of rhodamine B under visible-light irradiation. This research might provide a new approach to design novel nanocomposites.

2. EXPERIMENTAL

2.1. Synthesis of photocatalysts

The g-C_3N_4 was obtained according to the literature[16]. BiOCl/g-C_3N_4 composite was prepared through the hydrothermal method in the presence of SDBS. Briefly, 0.25 g of g-C_3N_4 powder was first dispersed in 80 mL of ethanol and sonicated for 2 h. After 0.2 g of SDBS has been added into g-C_3N_4 suspension, the obtained mixture were stirred for 1 h. After an appropriate amount of $BiCl_3$ were added into the obtained mixture, the mixture were vigorously stirred for 1 h. Then, the mixture were transferred into an autoclave with a PTEE container inside. The autoclave was maintained at 160 °C for 24 h. The products were washed with distilled water and absolute ethanol, respectively. Then, the obtained sample was dried at 60 °C for 6 h. The weight ratio of BiOCl:g-C_3N_4 was 1:1. Similarly, the pure BiOCl was prepared by the same procedure without addition of g-C_3N_4.

2.2 Characterization

The powder X-ray diffraction (Bruke D8 instrument with Cu K α (λ=0.15406 nm) was used to characterize the crystalline structures of the obtained samples. Infrared spectra were recorded with a NICOLET 5700 FTIR spectrometer. TEM images of the obtained samples was obtained by a JOEL JEM 2100F. X-ray photoelectron spectroscopy was recorded by an PHI-5000C ESCA system with Mg

Kα radiation. UV-vis absorption spectra of the obtained samples were performed on a Shimadzu UV-2550 spectrophotometer with $BaSO_4$ as the reference. Electrochemical impedance spectroscopy were carried out in three electrode with the CHI660E electrochemical workstation. Calomel electrodes and Platinum electrode served as the reference and counter electrode, respectively. The obtained samples modified electrode were used as the working electrode. The measurement was evaluated at the open-circuit potential. A sinusoidal ac perturbation of 5 mV was uesd to the electrode in the frequency range from 0.01 to 1×10^5 Hz.

2.3 Photocatalytic Reactions

Photocatalytic performance of the obtained samples were evaluated by the degradation of rhodamine B (RhB). The light source was obtained by The 300 W Xe lamp with a 400 nm cutoff filter was used as the visible light source. In each experiment, 50 mg of the catalyst was droped into 50 mL of rhodamine B solution (10 mg/L). Before irradiation, the solution was stirred for 30 min to reach the adsorption equilibrium between the catalyst and the solution. About 3 mL of solution was taken out at given time intervals. Concentrations of the obtained supernatant were analysed by an Unico UV-4802 spectrophotometer.

3. RESULTS AND DISCUSSION

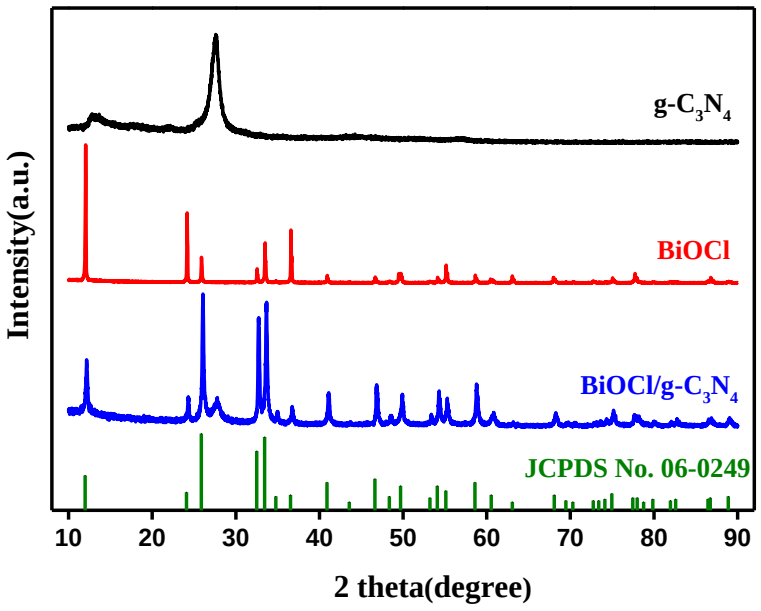

Figure 1. XRD pattern of g-C_3N_4, BiOCl and BiOCl/g-C_3N_4.

The crystal structure of the obtained samples was verified by X-ray powder diffraction (XRD) as shown in Figure 1. The bare g-C_3N_4 sample had two unique diffraction peaks at 13.1° and 27.4°, corresponding to the (1 0 0) and (0 0 2) planes of g-C_3N_4 (JCPDS card no. 87-1526) [16]. The bare BiOCl displayed the distinctive peaks at 2θ =11.9°, 24.1°, 25.9°, 32.5°, 33.4°, 36.5°, 40. 9°, 43.5°, 46.6°, 49.6°, 54.1°, 55.1°, 58.6°, and 77.9 °, corresponding to the (0 0 1), (0 0 2), (1 0 1), (1 1 0), (1 0 2), (0 0 3), (1 1 2), (1 0 3), (2 0 0), (1 1 3), (2 1 1), (1 0 4), (2 1 2), and (3 0 2) planes of tetragonal phase of BiOCl (JCPDS card no. 06-0249)[17]. These distinctive peaks were very obvious, suggesting a good crystallinity of the obtained BiOCl samples. Furthermore, the relative intensity of (001), (002) and (003) in the bare BiOCl sample were obviously higher than those in the standard spectrum. Moreover, the intensity of (001) was strongest among these facets, demonstrating the highly exposed (001) facet of BiOCl[18]. However, an obvious decrease in the intensity of (001), (002), and (003) peaks were found in the BiOCl/g-C_3N_4 material. Moreover, all diffraction peaks highly matched the standard spectrum [7, 8]. It can be known that the coupling between BiOCl and g-C_3N_4 play important roles in tailoring the oriented growth of the BiOCl crystal.

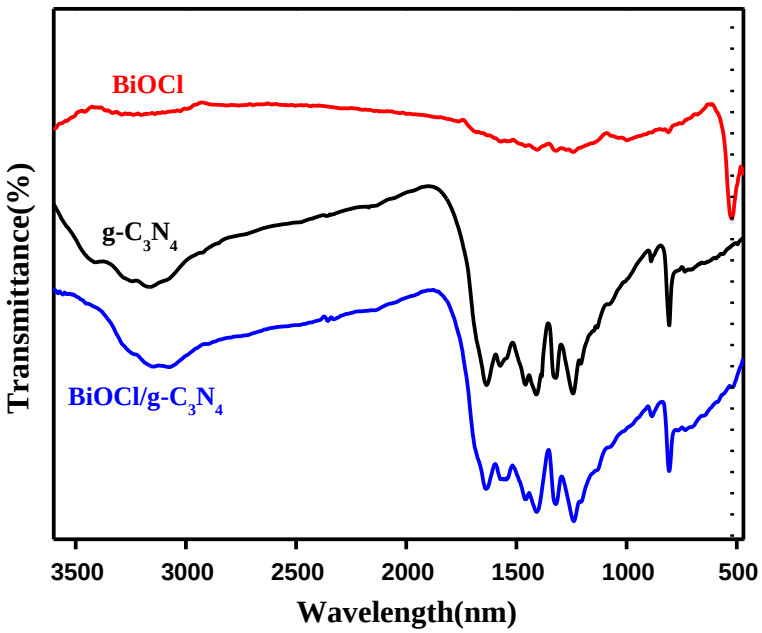

Figure 2. FT-IR spectra of g-C_3N_4, BiOCl and BiOCl/g-C_3N_4.

Figure 2 shows the FT-IR spectra of the the obtained samples. For the pure BiOCl sample, It could be seen that the absorption peak at 514 cm^{-1} was observed, which was evident from the Bi-O stretching mode[14]. For the g-C_3N_4 and BiOCl/g-C_3N_4, the absorption peaks at 1243, 1321 and 1402 cm^{-1} were assigned to stretching vibration modes of the aromatic C-N, and the peaks at 1640 cm^{-1} was suggested the stretching vibration modes of the C-N. Additionally, the peak at 809 cm^{-1} was indexed to the plane bending vibration modes of the s-triazine units[13, 14]. Furthermore, the intensity of absorption band at 514 cm^{-1} in BiOCl decrease significantly in the BiOCl/g-C_3N_4 compared with the

pure BiOCl, indicating an interaction between g-C_3N_4 and BiOCl. These results confirmed BiOCl and g-C_3N_4 had been coupled together successfully.

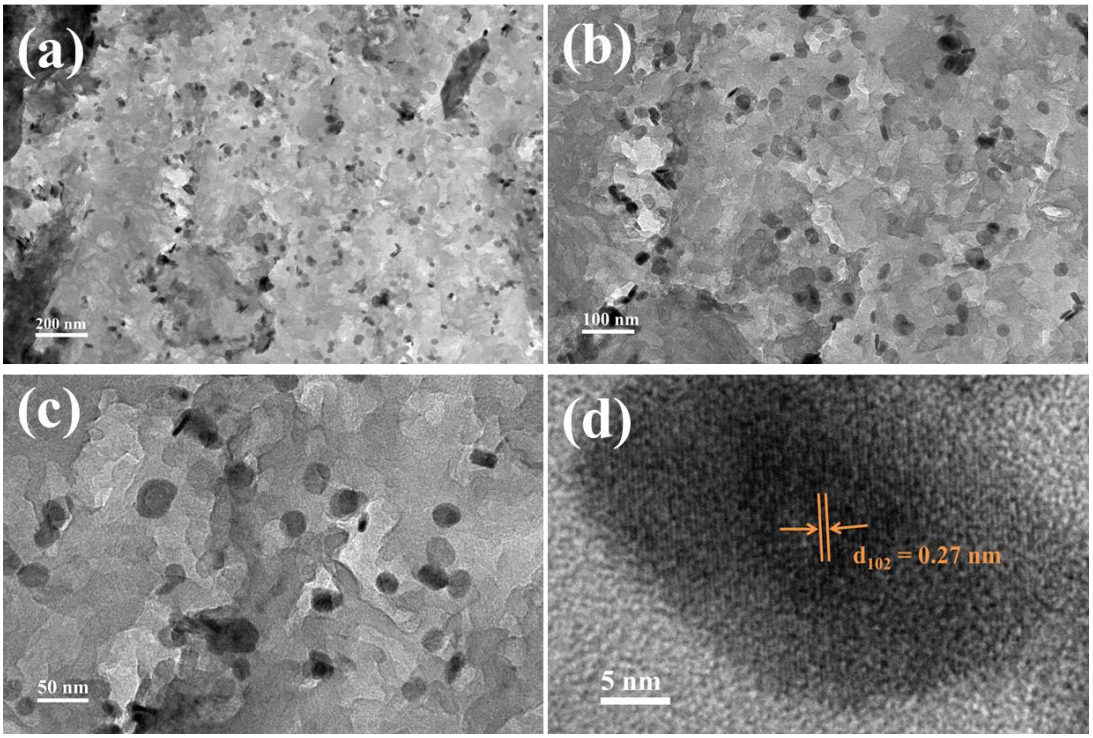

Figure 3. TEM (a-c) and HRTEM (d) images of the BiOCl/g-C_3N_4

Figure 3 shows the TEM and HRTEM images of the as-synthesized BiOCl/g-C_3N_4 sample. From the Figure 3a-c, BiOCl had a nanoplate-shaped structure with thickness below 5 nm and widths of 20 ~ 30 nm. These nanoplates were uniformly dispersed on the surface of g-C_3N_4. Moreover, the HRTEM image of the as-synthesized BiOCl/g-C_3N_4 (Figure 3d) revealed that the clear lattice fringe could be assigned to BiOCl, and the calculated d value of 0.27 nm corresponds to the (1 0 2) plane of BiOCl. This closely contacted the interfaces between g-C_3N_4 and BiOCl is good for the charge transfer between the two components, leading to an improved catalytic activity.

The elemental states of the BiOCl/g-C_3N_4 sample were further investigated by the XPS. Figure 4a was the survey XPS spectrum, which clearly indicated that the BiOCl/g-C_3N_4 was mainly composed of Bi, O, Cl, C, and N elements, and no other heteroelements were detected. The peaks at 164.3 and 159.0 eV could be ascribed to the Bi 4f 5/2 and Bi 4f 7/2 binding energies (Figure 4b), suggesting the existence of the Bi^{3+} in the crystal structure[17]. The Cl 2p XPS signals in Figure 4c was fitted into two peaks with binding energies at 198.1 and 199.6 eV, which could beascribed to Cl 2p 3/2 and Cl 2p 1/2 of Cl^- anions in BiOCl, respectively[17]. The O 1s XPS spectrum (Figure 4d) showed two major peaks at 532.2 and 530.3 eV, corresponding to the oxygen in BiOCl and the water molecules adsorbed in the sample [19]. For the C 1s in Figure 4e, the peaks appeared at 288.5 and 284.8 eV could be assigned to N=C-N groups and graphitic carbon of g-C_3N_4 [20]. The high-resolution XPS spectra of N 1s (Figure 4f) consist of three peaks at 398.5, 399.6, and 400.7 eV, which could be ascribed to C=N-C, N-C_3, and

N-H in g-C_3N_4, respectively[20]. The XPS spectra revealed the coexistence of g-C_3N_4 and BiOCl phases in the as-prepared heterostructure.

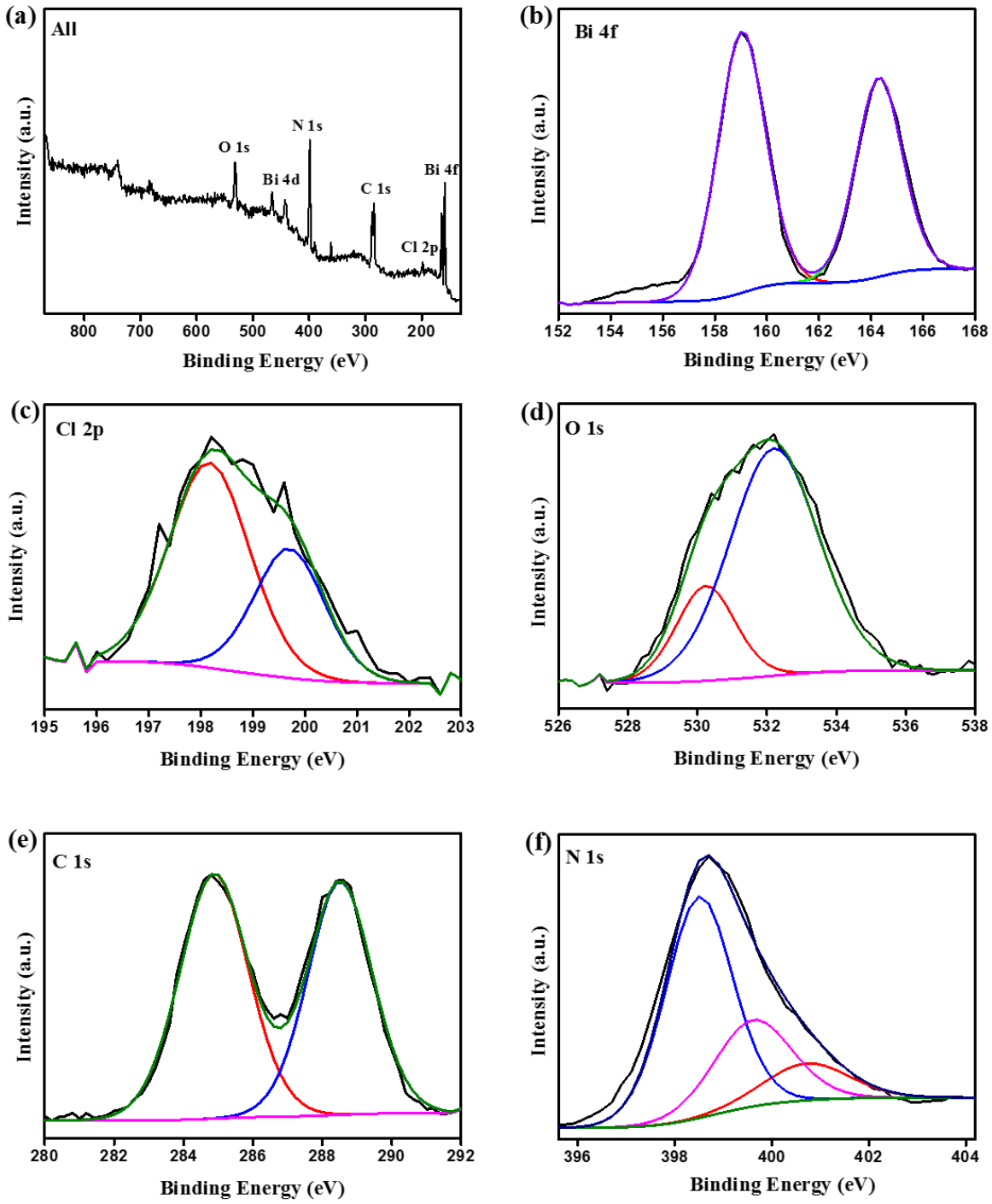

Figure 4. XPS spectra of survey spectrum (a), Bi 4f (b), Cl 2p (c), O 1s (d), C 1s (e), and N 1s (f) of the BiOCl/g-C_3N_4 sample.

The UV-vis diffuse reflectance spectroscopy of the as-synthesized samples are presented in Figure 5. The absorption edge of 460 nm was observed for the pristine g-C_3N_4[13]. The BiOCl sample

only had the photoabsorption in UV lightregion , and the absorption edge was 360 nm [7, 9]. After combining the two semiconductors, the BiOCl/g-C_3N_4 exhibited a wide visible-light absorption region and enhanced light absorption intensity in comparison with the bare BiOCl. It was confirmed that the BiOCl/g-C_3N_4 composite would be excited to produce more charge carriers, subsequently increased its photocatalytic activity.

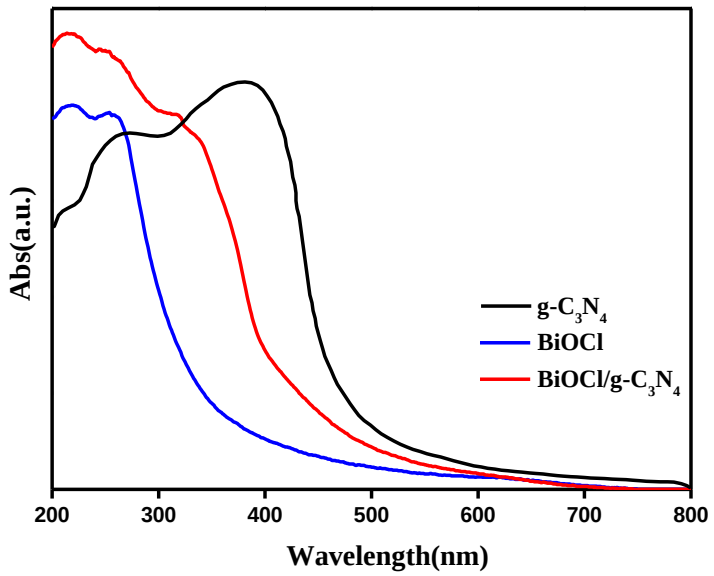

Figure 5. UV-vis diffuse reflectance spectra of g-C_3N_4, BiOCl and BiOCl/g-C_3N_4.

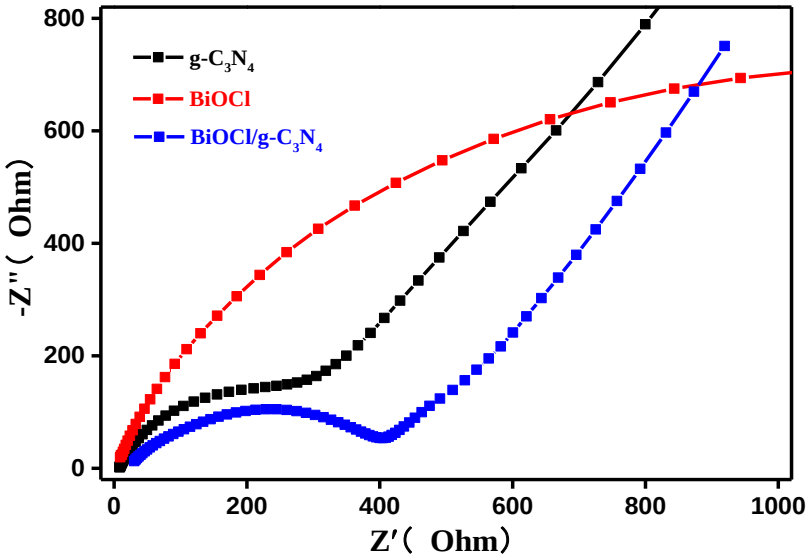

Figure 6. EIS Nyquist plots of g-C_3N_4, BiOCl and BiOCl/g-C_3N_4.

Electrochemical impedance spectroscopy (EIS) was an effective technique to analyze the transfer efficiency of charge carriers[21]. Generally, a smaller diameter of the EIS Nyquist plot means

an effective separation of charge carriers. So, the charge transfer process of the obtained samples were explored by EIS. EIS Nyquist plots of the prepared g-C_3N_4, BiOCl and BiOCl/g-C_3N_4 are shown in Figure 6. It was notable that the arc radius on EIS Nyquist plot of BiOCl/g-C_3N_4 sample was much smaller than that of the g-C_3N_4 and BiOCl sample. Therefore, the coupling between BiOCl and g-C_3N_4 dramatically improved the separation efficiency of charge carriers in the BiOCl/g-C_3N_4 sample.

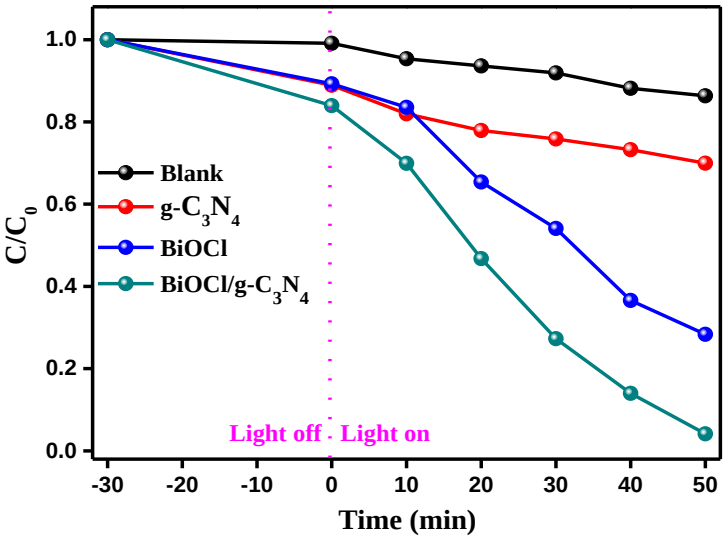

Figure 7. Photodegradation of RhB by g-C_3N_4, BiOCl and BiOCl/g-C_3N_4 under visible light.

The catalytic performance of the obtained samples were tested by the photodegradation of rhodamine B under visible light irradiation. As shown clearly in Figure 7, RhB was only slightly degraded with no catalysts, suggesting direct photolysis of RhB was negligible. With pure g-C_3N_4 and BiOCl as catalyst, the degradation rate of RhB can reach to 29.8 % and 72.6 % in 50 min, respectively. After combining the two semiconductors, the catalytic activity of the BiOCl/g-C_3N_4 composite was significantly improved compared with the pristine components. The remarkable catalytic property of BiOCl/g-C_3N_4 should be ascribed to the synergetic effects of light absorption and the interaction of heterojunction between BiOCl and g-C_3N_4.

4. CONCLUSION

In this work, the uniform BiOCl/g-C_3N_4 nanocomposite has been obtained via a facile solvothermal route with SDBS as the surfactant. TEM analysis indicated BiOCl nanoplates with widths of 20 ~ 30 nm and thickness below 5 nm are uniformly decorated on the surface of g-C_3N_4. The results demonstrated that BiOCl/g-C_3N_4 nanocomposite exhibits higher catalytic activity in the photodegradation of RhB than single BiOCl or g-C_3N_4. This research might provide a new approach to design novel nanocomposites.

ACKNOWLEDGEMENTS
This project was financially supported by Shanghai Jubo Energy Technology Co., Ltd and Yancheng Huanbo Energy Technology Co., Ltd, and the National Science Foundation of China (Grant No. 61171008).

References

1. C. Chen, W. Ma and J. Zhao, *Chem. Soc. Rev.*, 39 (2010) 4206.
2. J. Low, S. Cao and J. Yu, S. Wageh, *Chem. Commun.*, 50 (2014) 10768.
3. Y. Qu and X. Duan, *Chem. Soc. Rev.*, 42 (2013) 2568.
4. Y. Zheng, L. Lin, X. Ye, F. Guo and X. Wang, *Angew. Chem. Int. Edit.*, 53 (2014) 11926.
5. S. Banerjee, S.C. Pillai, P. Falaras, K.E. O'Shea, J.A. Byrne and D.D. Dionysiou, *J. Phys. Chem. Lett.*, 5 (2014) 2543.
6. Y.K. Huang, S.F. Kang, Y. Yang, H.F. Qin, Z.J. Ni, S.J. Yang and X. Li, *Appl. Catal. B-Environ.*, 196 (2016) 89.
7. Y. Mi, L.Y. Wen, Z.J. Wang, D.W. Cao, Y.G. Fang and Y. Lei, *Appl. Catal. B-Environ.*, 176 (2015) 331.
8. K. Zhang, D.Q. Zhang, J. Liu, K.X. Ren, H. Luo, Y.J. Peng, G.S. Li and X.B. Yu, *CrystEngComm*, 14 (2012) 700-707.
9. F. Cao, R.P. Deng, L.J. Huang, J. Ren, L.Q. Miao, J.M. Wang, S. Li and G.W. Qin, *Chem. Lett.*, 44 (2015) 1306.
10. H. Cheng, B. Huang and Y. Dai, *Nanoscale*, 6 (2014) 2009.
11. Y. Zheng, L. Lin, B. Wang and X. Wang, *Angew. Chem. Int. Edit.*, 54 (2015) 12868.
12. S.F. Kang, Y. Fang, Y.K. Huang, L.F. Cui, Y.Z. Wang, H.F. Qin, Y.M. Zhang, X. Li and Y.G. Wang, *Appl. Catal. B-Environ.*, 168 (2015) 472.
13. S. Shi, M.A. Gondal, A.A. Al-Saadi, R. Fajgar, J. Kupcik, X. Chang, K. Shen, Q. Xu and Z.S. Seddigi, *J. Colloid Interf. Sci.*, 416 (2014) 212.
14. J. Sun, J. Song, M.A. Gondal, S. Shi, Z. Lu, Q. Xu, X. Chang, D. Xiang and K. Shen, *Res. Chem. Intermed.*, 41 (2014) 6941.
15. D. Zhang, G. Li, H. Li and Y. Lu, *Chem. Asian J.*, 8 (2013) 26.
16. T.Y. Ma, S. Dai, M. Jaroniec and S.Z. Qiao, *Angew. Chem. Int. Edit.*, 53 (2014) 7281.
17. F. Chang, Y. Xie, J. Zhang, J. Chen, C. Li, J. Wang, J. Luo, B. Deng and X. Hu, *RSC Adv.*, 4 (2014) 28519.
18. D. Zhang, J. Li, Q. Wang and Q. Wu, *J. Mater. Chem. A.*, 1 (2013) 8622.
19. Q. Li, X. Zhao, J. Yang, C.J. Jia, Z. Jin and W. Fan, *Nanoscale*, 7 (2015) 18971.
20. Y. Li, K. Li, Y. Yang, L. Li, Y. Xing, S. Song, R. Jin and M. Li, *Chem. Eur. J.*, 21 (2015) 17739.
21. X.L. Yang, F.F. Qian, G.J. Zou, M.L. Li, J.R. Lu, Y.M. Li and M.T. Bao, *Appl. Catal. B-Environ.*, 193 (2016) 22.